bHLH121 and clade IVc bHLH transcription factors synergistically function to regulate iron homeostasis in Arabidopsis thaliana

Fei Gao, Meijie Li, Christian Dubos

HAL Id: hal-04592635

https://hal.inrae.fr/hal-04592635v1

Submitted on 29 May 2024

bHLH121 and clade IVc bHLH transcription factors synergistically function to regulate iron homeostasis in *Arabidopsis thaliana*

Fei Gao[1],[†], Meijie Li[1],[†], Christian Dubos[1],[*]

[1] IPSiM, Univ Montpellier, CNRS, INRAE, Institut Agro, Montpellier, France

[†] These authors contributed equally to this work

[*] Corresponding author (Tel: 0033 (0)499 61 28 18)

E-mails: Fei Gao, gaofei@hunau.edu.cn; Meijie Li, meijie.li@supagro.fr; Christian Dubos, christian.dubos@inrae.fr

Highlights

The master regulator bHLH121 act synergistically with clade IVc bHLH transcription factors to regulate iron homeostasis in Arabidopsis.

Abstract

Iron is an essential micronutrient for plant growth and development. In *Arabidopsis thaliana*, an intricate regulatory network involving several bHLH transcription factors (TFs) controls the homeostasis of iron. Among these TFs, bHLH121 plays a crucial role. bHLH121 interacts *in vivo* with clade IVc bHLH TFs and activates the expression of *FIT* and clade Ib bHLH TFs to stimulate the uptake of iron. How bHLH121 and clade IVc bHLH TFs function collectively and efficiently to maintain iron homeostasis is still unclear. Herein, we found that double loss-of-function mutants involving bhlh121 and one of the clade IVc bHLH displayed more severe iron deficiency associated growth defects than each of the single ones. We also found that among the four clade IVc bHLH TFs, solely *bHLH34* and *bHLH105* could partially complement the iron-associated growth defects of *bhlh121* when overexpressed. These data, together with protein localization analysis, support that bHLH121 and clade IVc bHLH TFs act synergistically to regulate iron homeostasis and that different bHLH121/clade IVc and clade IVc/clade IVc protein complexes are involved in this process.

Introduction

Iron is one of the most important microelements for almost all living organisms due to its key role in redox reactions. In plants, iron serves as cofactor for many enzymatic reactions and plays an irreplaceable role in vital processes, including DNA synthesis, hormone biosynthesis, respiration, photosynthesis and nitrogen fixation (Hänsch and Mendel, 2009). Although iron is abundant on earth, it is generally poorly available to the plants because it often exists in insoluble forms as iron(III) oxides and hydroxides, especially in neutral to basic soils. Therefore, iron might become a scarce resource and a limiting factor for plant growth and development, subsequently altering crop productivity and the quality of their derived products (Guerinot and Yi, 1994; Briat *et al*., 2015). However, redox-active iron can generate reactive oxygen species (ROS) through the Fenton reaction, which makes the plants also suffer from iron toxicity if iron availability is high (Briat *et al*,. 2010). Therefore, iron homeostasis in plants must be tightly controlled to integrate both the iron availability signals and the internal requirement.

To overcome the low iron solubility, plants have evolved two different strategies to acquire iron from the soil (Gao and Dubos, 2020; Marschner *et al*., 1986). Non-graminaceous species, including the model plant *Arabidopsis thaliana*, employ the reduction-based strategy (Strategy I), in which ferric iron (Fe^{3+}) is solubilized and mobilized through active proton (H^+) extrusion and coumarins secretion, reduced at the root surface and then transported into the rhizodermis cells as ferrous iron (Fe^{2+}) (Kobayashi and Nishizawa, 2012; Brumbarova *et al*., 2015; ; Fourcoy *et al*., 2016; Connorton *et al*., 2017; Robe *et al*., 2021a; Robe *et al*., 2021b). In Arabidopsis, these processes are ensured by the H^+-ATPase 2 (AHA2), the PLEIOTROPIC DRUG RESISTANCE 9 (PDR9) transporter, the FERRIC REDUCTION OXIDASE 2 (FRO2) and the IRON-REGULATED TRANSPORTER 1 (IRT1), respectively

(Robinson *et al*., 1999; Vert *et al*., 2002; Santi and Schmidt, 2009; Fourcoy *et al*., 2014; Robe *et al*., 2021a; Robe *et al*., 2021b). In chelation-based strategy (Strategy II), graminaceous plants biosynthesize and secrete high-affinity iron chelators, the phytosiderophores of the mugineic acid (MA) family, to chelate and directly acquire Fe(III) from soil (Kobayashi and Nishizawa, 2012; Kobayashi *et al*., 2014).

Iron deficiency can trigger the expression of genes responsible for iron uptake and translocation. These genes are tightly regulated at the transcriptional level by several transcription factors (TFs), which are critical for the maintenance of iron homeostasis in plants (Gao and Dubos, 2020; Gao *et al*., 2019). Several bHLH TFs have been identified and characterized as regulators of iron homeostasis in the past two decades (Gao and Dubos, 2020; Li et al., 2023). FIT (FER-LIKE IRON-DEFICIENCY-INDUCED TRANSCRIPTION FACTOR) was identified as a key regulator in driving Strategy I iron uptake machinery in Arabidopsis (Colangelo and Guerinot, 2004; Jakoby *et al*., 2004; Yuan *et al*., 2005). FIT interaction with the members of the clade Ib bHLH (i.e., bHLH38, bHLH39, bHLH100 and bHLH101) is required for the activation of its target genes, including *IRT1* and *FRO2* (Yuan *et al*., 2008; Wang *et al*., 2013). These interactions were also shown to enhance the stability of FIT (Cui *et al*., 2018).

Both *FIT* and clade *Ib bHLH* expression is induced by iron deficiency and is positively regulated by the clade IVc bHLH TFs, namely bHLH34 (also known as IDT1, IRON DEFICIENCY TOLERANT 1), bHLH104, bHLH105 (also known as ILR3, IAA-LEUCINE RESISTANT 3) and bHLH115 (Zhang *et al*., 2015; Li *et al*., 2016; Liang *et al*., 2017). The down regulation or the overexpression of clade IVc bHLH genes lead to decrease or increase of both *FIT* and clade *Ib bHLH* expression, respectively. Overexpression of clade IVc bHLH genes also results in iron overload (Zhang *et al*., 2015; Li *et al*., 2016; Liang *et al*., 2017). ChIP-qPCR and transactivation assays demonstrated that clade IVc bHLH TFs directly activate the expression of clade *Ib bHLH* genes and indirectly the expression of *FIT* via a yet unknow TF (Zhang *et al*., 2015; Li *et al*., 2016; Liang *et al*., 2017). Although clade IVc bHLH TFs shared the same target genes and showed similar molecular functions, it is likely they function in an additive manner to regulate the iron homeostasis since multiple loss-of-

function mutants show more severe iron deficiency symptoms than the single ones (Li *et al*., 2016; Liang *et al*., 2017).

Most recently, a bHLH transcription factor from the clade IVb, bHLH121 (also known as *URI*, *UPSTREAM REGULATOR OF IRT1*), has been identified and characterized as a key regulator of iron deficiency responses (Kim *et al*., 2019; Gao *et al*., 2020a; Gao *et al*., 2020b; Lei *et al*., 2020). *bhlh121* loss-of-function mutant displayed severe iron deficiency symptoms due to impaired iron deficiency responses and expression analysis indicated that bHLH121 is responsible for the induction of a set of iron-related genes including *bHLH38*, *bHLH39*, *bHLH100, bHLH101* and *FIT* under iron deficiency condition.

It is clearly demonstrated that bHLH121 interacts with all the members of the IVc bHLH clade (Gao *et al*., 2020a; Lei *et al*., 2020) and that clade IVc bHLH TFs can homo and heterodimerize (Zhang *et al*., 2015; Li *et al*., 2016; Liang *et al*., 2017). How bHLH121 and clade IVc bHLH proteins work collectively and efficiently to regulate the expression of their target genes, and thus iron homeostasis, still needs to be further investigated.

In this study, we found that double loss-of-function mutants between *bhlh121* and clade IVc *bhlh* TFs displayed more severe iron deficiency-associated growth defects compared to the single mutants. Consistent with this, expression analysis highlighted decreased iron deficiency responses in the double mutants when compared to single mutants. Constitutive expression of *bHLH34* and *bHLH105*, but not *bHLH104* or *bHLH115*, could partially complement the *bhlh121* iron deficiency symptoms notably by activating the expression of both clade Ib bHLH TFs and *FIT*. Last, protein localization studies also suggested that clade IVc bHLH TFs participate to the translocation of bHLH121 into the nucleus and demonstrated *in planta* that bHLH121 and clade IVc bHLH TFs accumulate in the same cells.

Altogether, the data generated in this study show that there is a bHLH121-independent function for the four clade IVc bHLH members in regulating the iron deficiency responses. In

addition, these data indicate that clade IVc bHLH TFs play distinct roles in the regulation of iron homeostasis that might be related to their specific expression pattern. Last, this study supports that bHLH121 and clade IVc bHLH TFs act synergistically to regulate iron homeostasis via the formation of different protein complexes.

Materials and methods

Plant material

Arabidopsis thaliana Columbia (Col-0) ecotype was used as the wild type. The *bhlh34* (GK-116E01), *bhlh104-1* (Salk_099496C)*, bhlh105/ilr3-3* (Salk_043690C)*, bhlh115-2* (WiscDsLox468D9) and *bhlh121-2* loss-of-function mutants have been described previously (Zhang *et al*., 2015; Li *et al*., 2016; Liang *et al*., 2017; Gao *et al*., 2020a). All the T-DNA insertion mutants were confirmed by PCR with gene-specific primers and left border primers of the T-DNA insertion. The *bhlh121 bhlh104*, *bhlh121 bhlh105* and the *bhlh121 bhlh115* double mutant plants were generated by crossing *bhlh121-2* as the male parent with *bhlh104-1, bhlh105/ilr3-3* and *bhlh115-2*, respectively. We failed to obtain the double *bhlh121-2 bhlh34* mutant by crossing because of the close proximity of both genes on the same chromosome. Therefore, we constructed the double mutant *bhlh121 bhlh34* by editing the *bHLH121* gene in the *bhlh34* mutant background by using the CRISPR/Cas9 technology. One representative allele was chosen for further investigation in this study. Sequencing analysis indicated that it contains a single nucleotide insertion (A) in exon 2 that is identical to the previously characterized *bhlh121-1* allele (Gao *et al*., 2020a). Single and double bhlh121 and clade IVc bHLH mutants were confirmed by RT-qPCR analysis (Fig. S1). The *bhlh121-2* mutant line complemented with the *ProbHLH121:gbHLH121-GFP* (translational fusion with the GFP, GREEN FLUORESCENT PROTEIN) construct is described elsewhere (Gao *et al*., 2020a). All the mutants were confirmed by sequencing. The primers used for genotyping are listed in Table S1.

Plant growth conditions

For *in vitro* cultures, seeds were surface sterilized using 12.5% bleach for 5 mins and rinsed 3 times with absolute ethanol. Sterilized seeds were plated on half-strength Murashige and Skoog (MS/2) medium containing 0.05% (w/v) MES (pH 5.7), 1% (w/v) sucrose and 0.7% (w/v) agar with different concentration of Fe-EDTA. For phenotypic analyses, plates were placed vertically in a growth chamber at 22°C under a long-day photoperiod (16 h light / 8 h dark) for 7 days. For the GUS staining assays, 7-day-old seedlings grown in presence of 50 μM iron (control) conditions were transferred to 0 μM iron plates (Fe deficiency condition) for another 7 days.

For hydroponic cultures, seeds were germinated on Hoagland medium containing 0.7% (w/v) agar with 50 μM Fe-EDTA. Plants were transferred to liquid Hoagland medium with 50 μM Fe-EDTA under short-day photoperiod (8 h light / 16 h dark) for 4 weeks (Fourcroy *et al*., 2016). For iron deficiency treatment, 5-week-old plants were rinsed with Milli-Q water 3 times and then transferred to liquid Hoagland medium in absence of iron for 1 week.

Plasmid construction and plant transformation

Arabidopsis Col-0 cDNAs were used as template to amplify the full length coding sequence (CDS with stop codons) of *bHLH34*, *bHLH104*, *bHLH105*, *bHLH115* and *bHLH121*. Purified PCR products were then inserted into the pDONR207 entry vector (BP Gateway reaction, Invitrogen) and subsequently recombined (LR Gateway reaction, Invitrogen) into the pUB-GFP binary destination vector downstream from the strong and ubiquitous promoter of the Arabidopsis *UBIQUITIN 10* (Grefen *et al*., 2010) to generate *bhlh121* overexpression lines. *bhlh121* lines overexpressing clade IVc bHLH TFs were confirmed by RT-qPCR analysis (Fig. S2).

To construct the *ProbHLH34:gbHLH34-GUS*, *ProbHLH104:gbHLH104-GUS*, *ProbHLH105:gbHLH105-GUS* and *ProbHLH115:gbHLH115-GUS* plants, 4328 bp, 3466 bp, 3557 bp, 3101 bp upstream from the stop codon of *bHLH34*, *bHLH104*, *bHLH105* and *bHLH115* were amplified and cloned into pDONR207, respectively. gDNA fragments were then recombined into the pGWB3 destination vector upstream from the *GUS* (*β-GLUCURONIDASE*) reporter gene or the pGWB4 vector upstream from the GFP (GREEN FLUORESCENT PROTEIN) (Nakagawa *et al*., 2007).

The *bHLH121* genomic fragment previously cloned into pDONR207 (Gao *et al*., 2020a) was recombined into the pGWB553 vector upstream from the RFP (RED FLUORESCENT PROTEIN) and pGWB3 destination vector upstream from the *GUS* (*β-GLUCURONIDASE*) reporter gene.

Agrobacterium tumefaciens strain GV3101 was used for transformation of WT or *bhlh121-2* plants through the floral dipping method (Clough and Bent, 1998). Seeds from T0 plants were selected on MS/2 agar plates containing 50 µg/ml hygromycin or 12.5 µg/ml glufosinate-ammonium for pGWB and pUB-GFP constructs, respectively. T3 homozygous lines were used for subsequent analyses. The primers used for cloning are listed in Table S1.

Co-transfection assays

For tobacco transient expression assays, the pB7FWG2 and pB7RWG2 vectors were used to generate the *Pro35S:bHLH-GFP* and *Pro35S:bHLH-RFP* constructs, respectively. The full length CDS without stop codons of *bHLH121* was amplified and cloned into the pB7FWG2, while the *bHLH34*, *bHLH104*, *bHLH105* and *bHLH115* were amplified and cloned into the pB7RWG2, respectively. The recombinant binary vector was mobilized into Agrobacterium strain GV3101. Agroinfiltration was performed in tobacco (*Nicotiana benthamiana*) leaves as described previously (Norkunas *et al*., 2018). Epidermal cells were observed by using laser scanning confocal microscopy (Leica TCS SP2 with Leica DM6000 microscope) after 48 hours post infiltration. Excitation laser wavelengths of 488 nm and 561 nm were used for imaging GFP and RFP signals, respectively.

Histochemical GUS staining

2-week-old seedlings expressing *ProbHLH34:gbHLH34-GUS*, *ProbHLH104:gbHLH104-GUS*, *ProbHLH105:gbHLH105-GUS*, *ProbHLH115:gbHLH115-GUS* and *ProbHLH121:gbHLH121-GUS* were collected and immersed immediately in 1 ml of GUS staining buffer [0.1 M phosphate buffer pH 7.5, 10 mM Na_2-EDTA, 0.1% (v/v) Triton X-100, 0.5 mM potassium ferricyanide, 0.5 mM potassium ferrocyanide and 2 mM X-Gluc (5-bromo-4-chloro-3-indolyl-β-D-glucuronide)]. The reaction was performed at 37°C overnight in the dark after a 1-hour vacuum treatment was applied at room temperature. After the

reaction, samples were rinsed with distilled water and treated with 70% (v/v) ethanol to remove the chlorophylls. Images were captured by using a motorized fluorescence stereo zoom microscope (ZEISS).

Gene expression analysis

Total RNA was extracted from about 100 mg fresh weight of 7-day-old seedlings by using Trizol reagent (Invitrogen). 1 μ g RNA was treated with DNase and then used for cDNA synthesis by using the RevertAid kit according to the manufacturer recommendations (Thermo Fisher Scientific). RT-qPCR analyses were performed by using ONEGreen® FAST qPCR Premix (Ozyme) on a LightCycler 480 real-time PCR system (Roche). *PROTEIN PHOSPHATASE 2A SUBUNIT A3* (*PP2AA3*) was used as internal control (Czechowski *et al*., 2005). Expression levels were calculated using the comparative threshold cycle method. The primers used for gene expression analysis are listed in Table S1.

Iron measurement

To measure iron concentration, leaves of 4-week-old plants grown in soils were harvested. Leaves and roots from plants grown in hydroponic culture were also separately harvested. Prior analysis, samples were dried at 65°C for 1 week in an oven. Ten milligrams of ground samples were homogenized with 750 μl of nitric oxide (65% [v/v]) and 250 μl of hydrogen peroxide (30% [v/v]). Following overnight incubation at room temperature, the samples were incubated at 85°C for 48 hours in a HotBlock (Environmental Express). Samples were then diluted by adding 4 ml Milli-Q water. Analysis of iron concentration was performed by MP-AES (Microwave Plasma Atomic Emission Spectroscopy, Agilent Technologies) analysis.

Chlorophyll measurement

Twenty milligrams of leaves (fresh weight) were collected and soaked overnight in 1 ml 100% acetone in the dark with strong shaking. The absorbance (A) of the supernatant was measured at 661.8 and 644.8 nm using a spectrophotometer (Beckman). Total chlorophyll contents were calculated as previously reported (Lichtenthaler, 1987).

Ferric chelate reductase (FCR) activity assays

FCR assays were performed as previously reported with slight modifications (Yi and Guerinot, 1996). Briefly, ten milligrams of fresh root tissues were soaked in 1 ml of FCR assays buffer (10 mM MES pH 5.5, 100 mM Fe^{3+}-EDTA and 300 mM ferrozine) for 1 hour in the dark. An identical assay without any root tissues was used as a blank. Samples were measured at 560 nm using a microplate reader (Xenius).

Statistical analysis

Initial raw data from experiments (i.e., root length, chlorophyll content, iron concentration, ferric-chelate reductase activity and RT-qPCR) were processed using Excel software (Microsoft Office). These processed data were used for statistical analysis using (i) one-way ANOVA (analysis of variance) with post-hoc Tukey HSD (honestly significant difference) with a level of significance set at $P \leq 0.05$ and (ii) Student t-test (means pairwise analysis) with a level of significance set at $P \leq 0.01$ and $P \leq 0.05$. All experiments made use of 3 replicates.

Accession Numbers

Sequence data in this study can be found in the GenBank/EMBL databases under the following accession numbers: bHLH121/URI (At3g19860); IRT1 (At4g19690); FRO2 (At1g01580); bHLH29/FIT (At2g28160); bHLH38 (At3g56970); bHLH39 (At3g56980); bHLH100 (At2g41240); bHLH101 (At5g04150); bHLH34 (At3g23210); bHLH104/IDT1 (At4g14410); bHLH105/ILR3 (At5g54680); bHLH115 (At1g51070); PP2AA3 (At1g13320).

Results

bHLH121 and clade IVc bHLH TFs double loss-of-function mutants display enhanced iron deficiency symptoms compare to the single mutants.

When grown in soil under greenhouse conditions, *bhlh121* mutant showed small stature and chlorotic leaves (Gao *et al*., 2020a) (Fig. 1A). In contrast, the four double mutants (i.e., *bhlh121 bhlh34*, *bhlh121 bhlh104*, *bhlh121 bhlh105* and *bhlh121 bhlh115*) displayed enhanced growth defects compare to the *bhlh121* single mutant (Fig. 1A). Both *bhlh121 bhlh104* and *bhlh121 bhlh105* double mutants withered and died early during their development when no extra iron was supplied (i.e., 1‰ Fe-EDDHA, ferric ethylenediamine di-(o-hydroxyphenylacetate), a form of iron easily assimilated by the plant; Fig. 1A). Without extra iron supply, the *bhlh121 bhlh34* double mutant displayed leaves with necrosis symptoms whereas the *bhlh121 bhlh115* mutant showed only smaller leaves compare to the *bhlh121* single mutant. In soil watered with 1‰ Fe-EDDHA, *bhlh121* and *bhlh121 bhlh115* were rescued and showed a similar phenotype to that of the wild type (WT). *bhlh121 bhlh34* displayed slight chlorosis symptoms in young leaves (Fig. 1A). The addition of 1‰ Fe-EDDHA improved *bhlh121 bhlh104* and *bhlh121 bhlh105* survival, but both double mutants still showed severe growth defects associated with leaves chlorosis and necrosis, which were more pronounced for the *bhlh121 bhlh105* double mutant (Fig. 1A).

Iron is indispensable for the biosynthesis of chlorophylls, and chlorophylls accumulation is a typical indicator of iron deficiency-associated leaves chlorosis (Terry, 1980). We measured the chlorophylls content of the different mutants grown in soil watered or not with exogenous iron (Fig. 1B). Under the control condition, there was no significant difference between the WT and the *bhlh34*, *bhlh104,* and *bhlh115* single mutants. In contrast, *bhlh121* and *bhlh105* were more chlorotic than the WT (Fig. 1B). *bhlh121 bhlh34*, *bhlh121 bhlh104* and *bhlh121 bhlh105* showed higher chlorosis defect than *bhlh121* (Fig. 1A). In contrast, no difference was observed between *bhlh121* and *bhlh121 bhlh115* (Fig. 1A). Chlorophyll content measurements confirmed these observations for *bhlh121 bhlh34* and *bhlh121 bhlh115* (Fig. 1B). In contrast, *bhlh121 bhlh104* and *bhlh121 bhlh105* chlorophyll content were not measured since both double mutants died too early during their development. When the plants were watered with exogenous iron (i.e., Fe-EDDHA), only the two double mutants

bhlh121 bhlh104 and *bhlh121 bhlh105* showed lower chlorophyll contents compare to the other genotypes (Fig. 1B).

We further investigated the phenotypes of plants grown on MS/2 medium containing different concentrations of iron. In the absence of iron (0 μM Fe), all the single mutants showed shorter root length compare to the WT (Fig. S3). *bhlh121 bhlh34*, *bhlh121 bhlh104* and *bhlh121 bhlh105* also displayed albinos cotyledons (Fig. S3 and S4). When the plants were grown under control condition (50 μM Fe), clade IVc bHLH single mutant grew and developed like the WT. In contrast, *bhlh121* single and double mutants still showed chlorotic cotyledons and shorter root length compared to the WT. At 200 μM iron (mild iron excess) and 500 μM Fe (iron excess), the root length of *bhlh121 bhlh105* was still shorter than that of all the other genotypes (Fig. S3 and S4).

Taken together, these results indicate that loss of function of IVc bHLH TFs in the *bhlh121* single mutant background enhances *bhlh121* iron deficiency-associated phenotypes, implying that bHLH121 and clade IVc bHLHs TFs play a synergistic role in the iron deficiency responses. It is noteworthy that among the clade IVc bHLH mutants alone or in combination with *bhlh121*, *bhlh105* displayed the strongest phenotype.

Loss of function of clade IVc bHLH TFs in *bhlh121* mutant causes decreased iron concentration.

To determine whether the loss of function of IVc bHLH in *bhlh121* causes altered iron concentration, we first measured the shoot iron concentration in 5-week-old WT and mutant plants grown in soil under greenhouse conditions. As shown in Fig. 1C, there was no significant difference between WT and *bhlh34* or *bhlh115* single mutant. In contrast, *bhlh121* single mutant and the *bhlh121 bhlh34* and *bhlh121 bhlh105* double mutants showed a lower iron concentration when compared to the WT plants (a decrease of about 21.8%, 42.3% and 31.7%, respectively). These results also highlighted that the *bhlh121 bhlh34* and *bhlh121 bhlh115* double mutants showed significantly lower iron concentration in the shoots compare to the *bhlh121* mutant (Fig. 1C). Iron concentration for the *bhlh121 bhlh104* and *bhlh121 bhlh105* double mutants was not measured since none of the plant survived without exogenous supply of iron.

To further investigate how the loss of function of clade IVc bHLH TFs in *bhlh121* mutant affects iron concentration in roots and shoots, WT and mutant plants were grown in hydroponic condition for 5 weeks and then subjected to iron deficiency (0 μM Fe) or kept in control (50 μM Fe) conditions for one additional week. Under control conditions, *bhlh121*, *bhlh34*, *bhlh121 bhlh34* and *bhlh121 bhlh115* showed decreased iron concentration compare to the WT in both shoots and roots (Fig. 2). In addition, a significant decrease in iron concentration was observed in the *bhlh121 bhlh34* and *bhlh121 bhlh115* double mutants compared to the corresponding single mutants in both shoots and roots. In contrast, *bhlh115* iron concentration was similar to that of the WT, in both shoots and roots. Interestingly, when plants were grown under the iron deficiency condition, there was no significant difference between the WT and the *bhlh121*, *bhlh34* and *bhlh115* mutants in the shoots. *bhlh121 bhlh34* and *bhlh121 bhlh115* double mutants showed lower iron concentrations in the shoots when compared to the corresponding single mutants (Fig. 2). In roots, *bhlh34* and *bhlh115* iron concentration was similar to that of the WT. By contrast, *bhlh121* and the double mutants (i.e., *bhlh121 bhlh34* and *bhlh121 bhlh115*) showed lower iron concentration. It is noteworthy that these three mutants accumulate iron at the same level (i.e., *bhlh121*, *bhlh121 bhlh34* and *bhlh121 bhlh115*). Together these results further support the synergistic functions of bHLH121 and the clade IVc bHLH TFs, in particular for the uptake of iron.

Loss of function of clade IVc bHLH TFs in *bhlh121* mutant enhances the impaired iron deficiency response.

To determine whether the decreased iron deficiency tolerance observed for the *bhlh121 bhlh34*, *bhlh121 bhlh104*, *bhlh121 bhlh105* and *bhlh121 bhlh115* double mutants was caused by the impaired expression of key iron deficiency-responsive genes, RT-qPCR experiments were conducted. For this purpose, seven-day-old seedlings were grown from germination under iron deficient and sufficient conditions and transcript accumulation of *IRT1*, clade Ib bHLH TFs (i.e., *bHLH38, bHLH39, bHLH100* and *bHLH101*) and *FIT* was analyzed.

As expected, the expression of *IRT1* was lower in the *bhlh121*, *bhlh34*, *bhlh104* and *bhlh105* single mutants compare to that of the WT under both iron deficient and sufficient conditions (Fig. 3 and S5). *IRT1* expression levels were also decreased in the *bhlh121 bhlh34, bhlh121*

bhlh104 and *bhlh121 bhlh105* double mutants when compared to the corresponding single mutants in both conditions. In contrast, no difference in *IRT1* expression levels was found between *bhlh121* and *bhlh121 bhlh115* double mutant when grown under iron deficiency. These observations suggest that the observed reduction in iron concentration in the double mutant is due to a decreased in iron uptake related to *IRT1* expression defects.

We also analyzed the expression of the Ib bHLH clade that are direct targets of clade IVc bHLH TFs (Zhang *et al*., 2015; Li *et al*., 2016; Liang *et al*., 2017). The expression of *bHLH39*, as well as *bHLH38* and *bHLH100*, was diminished in *bhlh121 bhlh34*, *bhlh121 bhlh104* and *bhlh121 bhlh105* double mutants when compared to the *bhlh121* single mutant when grown under the iron deficiency condition (Fig. 3 and S6). Similarly, the expression of *bHLH101* was lower in *bhlh121 bhlh34* and *bhlh121 bhlh104* double mutants when compared to *bhlh121* (Fig. S6). For the *bhlh121 bhlh115* double mutant, only the expression of *bHLH38* and *bHLH100* was lower than that of *bhlh121* (Fig. 3 and S6). As previously described, under iron sufficient condition, the expression of *bHLH100* and *bHLH101* in *bhlh121* was higher than in the WT (Gao et al. 2020a) and similar to that of the double mutants (except for *bhlh121 bhlh105*; Fig. S7).

Under iron deficiency condition, all the double mutant but *bhlh121 bhlh105* showed no significant difference in the transcript abundance of *FIT* with the *bhlh121* single mutant (Fig. 3). When the plants were grown under the control condition, no variation in *FIT* expression was found between the *bhlh121*, *bhlh34*, *bhlh104*, *bhlh105* and *bhlh115* mutants and the WT. Interestingly, the expression of *FIT* was strongly diminished in all four double mutants.

Altogether, these results suggest that bHLH121 and the clade IVc bHLH TFs play an synergistic role in regulating the expression of clade Ib bHLH TFs and *FIT*, and thus *IRT1* and the uptake of iron.

Overexpression of *bHLH34* and *bHLH105* partially rescues the iron-deficiency phenotype of *bhlh121* mutant.

Previous studies showed that the overexpression of clade *IVc bHLH* TFs in WT plants could result in enhanced iron deficiency tolerance and over-accumulation of iron (Zhang *et al*., 2015a; Li *et al*., 2016a; Liang *et al*., 2017). To determine whether bHLH121 is required for these activities, the four clade *IVc bHLH* TFs were overexpressed in the *bhlh121* mutant.

Two representative transgenic lines per clade *IVc bHLH* displaying increased expression level were chosen for further analysis (Fig. S2). When the plants were grown in soil under the greenhouse condition, the *bhlh121* mutant lines overexpressing *bHLH104* and *bHLH115* (*ProUBI::bHLH104* in *bhlh121* and *ProUBI::bHLH115* in *bhlh121*) displayed similar phenotype to that of *bhlh121* mutant, showing small stature and chlorotic leaves (Fig. 4A). There was also no significant difference in chlorophyll contents (Fig. 4B). In contrast, overexpression of *bHLH34* and *bHLH105* (*ProUBI::bHLH34* in *bhlh121* and *ProUBI::bHLH105* in *bhlh121*) partially rescued the iron-associated phenotypes of *bhlh121* mutant. For instance, both lines showed bigger leaves and higher chlorophylls content than those of the *bhlh121* mutant (Fig. 4A and B).

Similar results were obtained when plants were grown *in vitro*. *ProUBI::bHLH34* in *bhlh121* and *ProUBI::bHLH105* in *bhlh121* lines showed stronger tolerance to iron deficiency than *bhlh121*. These overexpression lines had longer roots than the *bhlh121* mutant plants, but shorter roots than the WT under low iron conditions (0, 10 and 25 μM) (Fig. S8 and S9). However, neither *bHLH104* nor *bHLH115* overexpression was able to overcome the *bhlh121* growth defects. *ProUBI::bHLH104* in *bhlh121* and *ProUBI::bHLH115* in *bhlh121* lines showed similar root length than *bhlh121* under the different iron conditions that were tested (0, 10, 25 and 50 μM) (Fig. S8 and S9). These phenotypic analyses showed that the overexpression of *bHLH34* and *bHLH105*, but not *bHLH104* and *bHLH115*, could partly complement the iron-associated phenotype of *bhlh121* mutant, indicating that the four clade IVc bHLH members play distinct roles in the regulation of iron homeostasis.

To further investigate how the overexpression of clade *IVc bHLH* TFs in *bhlh121* mutant affects iron concentration in roots and shoots, we grew plants in hydroponic condition and subjected them or not to iron deficiency (Fig. S10). In roots, overexpression of *bHLH34* and *bHLH105* increased the iron concentration in the *bhlh121* mutant regardless of whether the plants were grown in the presence or absence of iron (Fig. 5A). Such an increase was also observed in the shoots of these overexpression lines grown under control conditions, whereas no difference was detected in this tissue when grown under iron deficiency conditions. In agreement with the phenotypic analysis, overexpression of *bHLH104* and *bHLH115* in *bhlh121* showed no significant effect on the concentration of iron, neither in the roots nor in the shoots.

In addition, to further investigate how the overexpression of clade *IVc bHLH* TFs in *bhlh121* mutant affects iron homeostasis, the ferric-chelate reductase (FCR) activity was analyzed (Yi and Guerinot, 1996). As shown in Fig. 5B, overexpression of *bHLH34* and *bHLH105* in *bhlh121* increased the FCR activity. These results suggest that bHLH34 and bHLH105 can partly reconstitute the iron uptake system to promote plant iron nutrition in the absence of bHLH121.

Overexpression of *bHLH34* and *bHLH105* activates the expression of both *FIT* and clade Ib bHLH TFs in *bhlh121* mutant.

Previous studies showed that overexpression of clade IVc bHLH in WT plants could constitutively activate the iron deficiency response genes regardless of the iron status (Zhang *et al.*, 2015a; Li *et al.*, 2016a; Liang *et al.*, 2017). In this study we found that overexpression of *bHLH34* and *bHLH105* partially complemented the iron deficiency phenotypes of *bhlh121*. Whether or not this observation was due to the activation of key downstream components of the iron deficiency regulatory network was still to be determined. For this purpose, the expression of *IRT1*, clade Ib bHLH TFs, and *FIT* in these overexpression lines was analyzed by RT-qPCR.

Expression analyses indicated that the overexpression of *bHLH34* and *bHLH105* increased the expression of *IRT1* to a level similar to that of the WT under iron sufficient condition (Fig. S11). Under iron deficiency condition, the expression of *IRT1* was induced, although the expression level was still lower compared to the WT (Fig. 6). By contrast, overexpression of *bhLH104* and *bHLH115* did not affect *IRT1* expression in the absence of bHLH121 in both conditions (Fig. 6 and S10). These expression data are in agreement with the iron concentration measurements (Fig. 5A).

Overexpression of *bHLH34*, *bHLH104* and *bHLH105* could restore the expression of *bHLH39*, as well as *bHLH38* and *bHLH101*, in *bhlh121* mutant under iron deficiency conditions. (Fig. 6 and S12). Similarly, the expression of *bHLH101* was restored in *bhlh121* lines overexpressing *bHLH34* and *bHLH104* but not in lines overexpressing *bHLH105* and *bHLH115* (Fig. S12). For the *bhlh121* lines overexpressing *bHLH34*, the expression of *bHLH39* and *bHLH100* was also restored but not the one of *bHLH38* (Fig. 6 and S12). Last, overexpression of *bHLH115* restored the expression of bHLH39 and to a lesser extend the

expression of *bHLH38* and *bHLH100* (Fig. 6 and S12). Under Fe sufficient condition, mRNA levels of *bHLH38* and *bHLH39* was overall higher in the overexpressing lines than in the *bhlh121* and similar or higher than that the WT (Fig. S11 and S13). The expression of *bHLH100* and *bHLH101* was higher in the overexpressing lines than in the WT and similar or lower than *bhlh121* (Fig. S13). These results indicate that bHLH121 and clade IVc bHLH TFs play redundant roles, to a certain extent, in activating the expression of clade *Ib bHLH* TFs.

Overexpression of *bHLH34* and *bHLH105* rescued as well the expression of *FIT* in the *bhlh121* mutant background under both iron deficient and sufficient conditions (Fig. 6 and S8). In contrast, overexpression of *bHLH104* and *bHLH115* showed no effect on the expression of *FIT*.

Taken together, these results suggest that the overexpression of *bHLH34* and *bHLH105* (and not *bHLH104* and *bHLH115*) is sufficient to activate both *FIT* and clade Ib bHLH expression that in turn activate the expression of genes involved in iron uptake such as *IRT1*.

bHLH121 and clade IVc bHLH TFs show different but complementary expression patterns in roots.

Given the potential synergistic roles of bHLH121 and clade IVc bHLH TFs in regulating the iron deficiency responses, we investigated whether the expression pattern of these TFs were different or not. To achieve this goal, we constructed the *ProbHLH121:gbHLH121-GUS*, *ProbHLH34:gbHLH34-GUS*, *ProbHLH104:gbHLH104-GUS*, *ProbHLH105:gbHLH105-GUS* and *ProbHLH115:gbHLH115-GUS* transgenic lines.

GUS staining results revealed that *bHLH121*, *bHLH34*, *bHLH104*, *bHLH105* and *bHLH115* were expressed in both roots and shoots and shared similar tissue expression patterns in leaves (Fig. 7). All plants showed stronger GUS activity in cotyledons and young leaves compared with the older ones. In the hypocotyls, strong GUS activities were detected for the *ProbHLH104:gbHLH104-GUS* and *ProbHLH105:gbHLH105-GUS* lines, but not for the *ProbHLH121:gbHLH121-GUS*, *ProbHLH34:gbHLH34-GUS* and *ProbHLH115:gbHLH115-GUS* ones.

In the roots, all the studied lines displayed GUS activity in the root tips and the elongation zone of both primary and lateral roots (Zone IV). In addition, GUS activity was observed for *bHLH121*, *bHLH104*, *bHLH105* and *bHLH115* in the root maturation zone (Zone III). For *bHLH104* and *bHLH105* GUS activity was also detected in the stele of the upper part of the root system, below the hypocotyl (Zone I) and in the area with fully developed lateral roots (Zone II) (Fig. 7).

The different tissue-specific expression patterns observed for *bHLH121* and the clade IVc bHLH TFs in the roots suggest that these proteins might have redundant activities in some tissues (e.g., root tip, root elongation zone, leaves) and more specific ones in some others (e.g., mature roots, hypocotyl). This assertion is in adequacy with the synergistic role observed for these TFs in regulating the plant iron deficiency responses (Li *et al*., 2016a) (Fig. S14).

Clade IVc bHLH TFs act redundantly to target bHLH121 into the nucleus.

bHLH121 and clade IVc bHLH TFs were shown to interact *in vivo*, in both yeast and Arabidopsis cells (Gao et al. 2020a; Lei et al. 2020). Transient expression assays conducted in tobacco cells suggested that the specific accumulation of bHLH121 into the nucleus was depending on clade IVc bHLH TF activities (Lei et al. 2020). In this study, bHLH121 fused to the m-Cherry fluorescent protein was found to localize into the nucleus and the cytoplasm when expressed alone. In contrast, when co-expressed with clade IVc bHLH TFs fused to the GFP, mCherry fluorescence was no longer observed in the cytoplasm and bHLH121-mCherry accumulation was restricted to the nucleus where it colocalized with GFP signal (Lei *et al*., 2020). Here, we confirm these observations by conducting a similar experiment using different vectors in which bHLH121 was fused to the GFP and clade IV bHLH TFs to the RFP (Fig. 8A and S15). It is noteworthy that in our experiments, we observed a strong decrease of bHLH121-GFP signal in the cytoplasm but not a full disappearance that might be due to differences in the systems used.

To determine whether the absence of clade IVc bHLH TFs could affect the nuclear localization of bHLH121 in Arabidopsis, we introduced the *ProbHLH121:gbHLH121-GFP* construct into the four clade IVc bHLH single mutants (i.e., *bhlh34*, *bhlh104*, *bhlh105* and *bhlh115*). This was achieved by crossing these mutants with a *bhlh121-2* mutant line carrying

the *ProbHLH121:gbHLH121-GFP* transgene (Gao *et al*., 2020). As shown in Fig. 8B and S16, confocal microscopy revealed that all lines displayed bHLH121-GFP fluorescence in the nucleus of root cells, suggesting a redundant role for clade IVc bHLH TFs in promoting the nuclear localization of bHLH121 in roots.

In order to validate this hypothesis, transgenic lines expressing both *ProbHLH121:gbHLH121-RFP* and *ProbHLH34:gbHLH34-GFP*, *ProbHLH121:gbHLH121-RFP* and *ProbHLH104:gbHLH104-GFP*, *ProbHLH121:gbHLH121-RFP* and *ProbHLH105:gbHLH105-GFP* or *ProbHLH121:gbHLH121-RFP* and *ProbHLH115:gbHLH115-GFP* were generated. The analysis of these stably transformed plants by confocal microscopy showed that in roots, bHLH121 colocalized with bHLH104, bHLH105 and bHLH115 in the nucleus of the same cells (Fig. 8C and S17), which was in adequacy with our GUS analysis (Fig. 7). No conclusion was made for the colocalization study between bHLH121 and bHLH34 since the GFP signal was too weak (data not shown).

Discussion

The transcriptional activity of a given bHLH TF relies on its ability to form homo- and/or hetero-dimers. bHLH121, that is a key regulator of the iron deficiency responses form heterodimers with the bHLH TFs belonging to clade IVc (Gao *et al*., 2020a, Lei *et al*., 2020). Each single loss-of-function mutant for *bHLH121* and clade IVc bHLH TFs showed sensitivity to iron deficiency, including chlorotic leaves and defects in primary root development (Zhang *et al*., 2015a; Li *et al*., 2016a; Liang *et al*., 2017; Kim *et al*., 2019; Gao *et al*., 2020a; Lei *et al*., 2020). Multiple loss-of-function mutants for the clade IVc bHLH TFs (i.e., *bhlh34 bhlh104*, *bhlh104 bhlh115* and *bhlh105 bhlh115*) displayed stronger growth defects under iron deficiency than the parental single mutants, indicating the non-redundant but additive role of clade IVc bHLH TFs in the regulation of iron homeostasis (Li et al. 2016; Liang et al. 2017).

It was reported that the phenotypes of *bhlh121 bhlh104* and *bhlh121 bhlh115* double mutants were similar to that of the *bhlh121-5* single mutant and they concluded that bHLH121 acts downstream of clade IVc bHLH in the Fe homeostasis network (Lei et al. 2020). In contrast, in the present study we found that *bhlh121 bhlh34*, *bhlh121 bhlh104*, *bhlh121 bhlh105* and *bhlh121 bhlh115* double mutants showed enhanced growth defects compare to the *bhlh121* mutant under both iron deficiency and sufficient conditions. These discrepancies may be due to the different genetic backgrounds of the *bhlh121* mutant used in these two studies. The *bhlh121-5* mutant encodes a truncated bHLH121 protein that contains a complete bHLH domain that is required for the heterodimerization with other bHLH TFs, whereas *bhlh121-2* mutant backgrounds encode truncated bHLH121 protein with an incomplete bHLH domain. This hypothesis is further supported by the fact that three *bhlh121* mutant alleles affected in their bHLH domain (i.e., *bhlh121-2*, *bhlh121-1* and *bhlh121-4*) showed stronger growth defects than *bhlh121-5* when grown in soil (Gao *et al*., 2020a; Lei *et al*., 2020). In our study, we also determined the iron-associated phenotypes of the double mutants under two different growth conditions (i.e., in soil and in *vitro*) and provided compelling evidence to show that these double mutants presented stronger growth defects than the *bhlh121* single mutants (Fig. 1, S3 and S4). Furthermore, we demonstrated that the iron concentrations are lower in *bhlh121 bhlh34* and *bhlh121 bhlh115* double mutants when compared to *bhlh121* single mutants (Fig. 1 and 2).

bHLH121 and clade IVc bHLH TFs share a set of target genes, including *FIT* and clade Ib bHLH (Zhang *et al*., 2015; Li *et al*., 2016; Liang *et al*. 2017; Kim *et al*., 2019; Gao *et al*., 2020). The expression of *FIT* and clade Ib bHLH is decreased in the *bhlh121*, *bhlh34*, *bhlh104*, *bhlh105* and *bhlh115* single mutants. In addition, their expression levels in *bhlh34 bhlh104*, *bhlh34 bhlh105* and *bhlh104 bhlhl105* double mutant was shown to be lower than that of the single mutants, suggesting non-redundant but additive roles for the clade IVc bHLH TFs in the transcriptional regulation of these genes (Li *et al*., 2016,). Herein, we confirmed that the expression of the clade Ib bHLH genes was drastically reduced in *bhlh121* mutant under iron deficiency and found that clade Ib bHLH expression was even lower in the *bhlh121* double mutants (except *bHLH101* in *bhlh121 bhlh105* and *bHLH39* and *bHLH101* in *bhlh121 bhlh115*) (Fig. 3 and S6). These observations indicate that if bHLH121 and clade IVc bHLH heterodimers are the main TF complexes regulating clade Ib bHLH expression, there are clade IVc bHLH complexes that are also at play in this regulation. In addition, it

also suggests that there might be a threshold level of clade IVc bHLH TFs under which clade Ib bHLH expression is nearly abolished and that is reached when clade IVc bHLHs are mutated in the *bhlh121* background. In contrast, the expression of *FIT* was only reduced in *bhlh121 bhlh105* double mutant, but not in the other ones, compared to the single *bhlh121* mutants. Similarly, the expression of *FIT* is most affected in *bhlh105* single mutant than in the other clade IVc bHLH single mutants. Together, these observations support that among the clade IVc bHLH TFs, bHLH105 might play a preponderant role in regulating the expression of *FIT* under iron deficiency conditions.

Overexpression of *bHLH104* and clade *bHLH115* could activate the expression of clade Ib bHLH (except for *bHLH101* in the *bHLH115* overexpressing lines) but not the expression of *FIT* in the *bhlh121* mutant, which is not sufficient to activate *IRT1* expression to facilitate the uptake of iron and thus complement *bhlh121* growth defects. These observations were in adequacy with similar experiments conducted in a previous study (Lei *et al*., 2020). By contrast, overexpression of *bHLH34* and *bHLH105* could partially complement the iron-associated phenotype (including the FCR activity and the concentration of iron) of *bhlh121* by up-regulating the expression of both clade Ib bHLH (except for *bHLH101* in the *bHLH105* overexpressing lines) and *FIT* (Fig. 5, 6 and S12). Since *FIT* is not a direct target of clade IVc bHLH TFs (Zhang *et al*., 2015; Li *et al*., 2016), these results imply the existence of other transcription factors to connect *FIT* expression with bHLH34 and bHLH105 activities. In this experiment, it was also surprising to observe that the closest bHLH homologs from clade IVc (i.e., bHLH34 and bHLH104 on one hand and bHLH105 and bHLH115 on the other; Long *et al*., 2010) do not fully share the same target genes.

One possible mechanistic basis for the differential control of shared target genes by the individual above described bHLH TFs (i.e., bHLH121 and clade IVc bHLH TFs) is that each bHLH TF has a different spatial expression pattern within the plant body. Previous promoter-GUS analyses revealed that *bHLH038*, *bHLH039* and *bHLH100* were expressed in shoots and roots (Wang *et al*., 2007). Within roots, GUS activity was detected in the epidermis and inside the root except near the root tip. In contrast to that, GUS activity driven by the promoter of *FIT* was specifically expressed in roots near the root tip and also in the upper root zones under iron deficiency condition (Colangelo and Guerinot, 2004; Jakoby *et al*.,

2004). Thus, the *FIT* expression pattern overlapped with those of clade Ib bHLH genes within the root except near the root tip (Wang *et al*., 2007; Jakoby *et al*., 2004). We found that bHLH121 and clade IVc bHLH display in roots different pattern of accumulation (Fig. 7). bHLH121, bHLH104, bHLH105 and bHLH115 are localized in the maturation zone (Zone III), where the *FIT* and clade Ib bHLH TFs also showed strong expression under iron deficiency conditions. These observations support that bHLH121 and IVc bHLH TFs (except bHLH34) function coordinately to regulate the expression of *FIT* and clade Ib bHLH TFs within these regions. In addition, at the upper maturation zone (Zone I and II), only bHLH104 and bHLH105 accumulate in the stele, implying some putative function in iron homeostasis extending beyond the uptake of iron. These results could partially explain why the *bhlh121 bhlh104* and the *bhlh121 bhlh105* double mutants showed the most severe growth defect among the four double mutants that were analyzed. It is noteworthy that bHLH121 and clade IVc bHLH TFs are also expressed in the shoots, especially in the veins (Li *et al*., 2016; Liang *et al*., 2017; Lei *et al*., 2020) (Fig. 7). Since *YSL3* (*YELLOW STRIPE LIKE 3*) and *OPT3* (*OLIGOPEPTIDE TRANSPORTER 3*)*,* two iron transport and mobilization related genes, are highly expressed in the veins (Waters *et al*., 2006; Stacey *et al*., 2008; Mendoza-Cózatl *et al*., 2014; Zhai *et al*., 2014) and are direct targets of bHLH121 (Kim et al., 2019), it might be that the function of bHLH121 and clade IVc bHLH TFs in aerial tissues would be to modulate iron transport and partitioning.

Taken together, the data presented herein demonstrate that bHLH121 and clade IVc act synergistically to regulate iron homeostasis and that different bHLH121/clade IVc and clade IVc/clade IVc protein complexes are involved in this process (Fig. 9).

Acknowledgements

Author contributions

FG and CD conceived and designed the experiments, analyzed the data and wrote the manuscript, FG and ML performed the experiments and CD contributed reagents/materials/analysis tools.

Data availability statement

All data supporting the findings of this study are available within the paper and within its supplementary materials published online.

References

Briat J-F, Dubos C, Gaymard F. 2015. Iron nutrition, biomass production, and plant product quality. Trends in Plant Science 20, 33-40

Briat J-F, Duc C, Ravet K, *et al*. 2010. Ferritins and iron storage in plants. Biochimica et Biophysica Acta (BBA)-General Subjects 1800, 806-814

Brumbarova T, Bauer P, Ivanov R. 2015. Molecular mechanisms governing Arabidopsis iron uptake. Trends in Plant Science 20, 124-133

Clough SJ, Bent AF. 1998. Floral dip: a simplified method for Agrobacterium‐mediated transformation of Arabidopsis thaliana. The plant journal 16, 735-743

Colangelo EP, Guerinot ML. 2004. The Essential Basic Helix-Loop-Helix Protein FIT1 Is Required for the Iron Deficiency Response. The Plant Cell 16, 3400-3412

Connorton JM, Balk J, Rodríguez-Celma J. 2017. Iron homeostasis in plants‐a brief overview. Metallomics 9, 813-823

Cui Y, Chen C-L, Cui M, *et al*. 2018. Four IVa bHLH transcription factors are novel interactors of FIT and mediate JA inhibition of iron uptake in Arabidopsis. Molecular plant 11, 1166-1183

Czechowski T, Stitt M, Altmann T *et al*. 2005. Genome-wide identification and testing of superior reference genes for transcript normalization in Arabidopsis. Plant physiology 139, 5-17

Fourcroy P, Tissot N, Gaymard F, *et al*. 2016. Facilitated Fe nutrition by phenolic compounds excreted by the Arabidopsis ABCG37/PDR9 transporter requires the IRT1/FRO2 high-affinity root Fe2+ transport system. Molecular plant 9, 485-488

Gao F, Dubos C. 2021. Transcriptional integration of the plant responses to iron availability. Journal of Experimental Botany 72, 2056-2070

Gao F, Robe K, Bettembourg M, *et al*. 2020a. The Transcription Factor bHLH121 Interacts with bHLH105 (ILR3) and Its Closest Homologs to Regulate Iron Homeostasis in Arabidopsis. The Plant Cell 32, 508-524

Gao F, Robe K, Dubos C. 2020b. Further insights into the role of bHLH121 in the regulation of iron homeostasis in Arabidopsis thaliana. Plant Signaling and Behavior 15, 1795582.

Gao F, Robe K, Gaymard F, *et al*. 2019 The transcriptional control of iron homeostasis in plants: a tale of bHLH transcription factors? Frontiers in plant science 10, 6

Grefen C, Donald N, Hashimoto K, *et al*. 2010. A ubiquitin‐10 promoter‐based vector

set for fluorescent protein tagging facilitates temporal stability and native protein distribution in transient and stable expression studies. The Plant Journal 64, 355-365

Guerinot ML, Yi Y. 1994. Iron: Nutritious, Noxious, and Not Readily Available. Plant Physiology 104, 815-820

Hänsch R, Mendel RR. 2009. Physiological functions of mineral micronutrients (cu, Zn, Mn, Fe, Ni, Mo, B, cl). Current opinion in plant biology 12, 259-266

Jakoby M, Wang H-Y, Reidt W, *et al*. 2004. FRU (BHLH029) is required for induction of iron mobilization genes in Arabidopsis thaliana. FEBS letters 577, 528-534

Kim SA, LaCroix IS, Gerber SA, *et al*. 2019. The iron deficiency response in Arabidopsis thaliana requires the phosphorylated transcription factor URI. Proceedings of the National Academy of Sciences 116, 24933-24942

Kobayashi T, Itai RN, Nishizawa NK. 2014. Iron deficiency responses in rice roots. Rice 7, 27

Kobayashi T, Nishizawa NK. 2012. Iron uptake, translocation, and regulation in higher plants. Annual review of plant biology 63, 131-152

Lei R, Li Y, Cai Y, *et al*. 2020. bHLH121 Functions as a Direct Link that Facilitates the Activation of FIT by bHLH IVc Transcription Factors for Maintaining Fe Homeostasis in Arabidopsis. Molecular Plant 3, 634-649

Li M, Watanabe S, Gao F, *et al*. 2023. Iron Nutrition in Plants: Towards a New Paradigm? Plants (Basel) 12, 384.

Li X, Zhang H, Ai Q, *et al*. 2016. Two bHLH transcription factors, bHLH34 and bHLH104, regulate iron homeostasis in Arabidopsis thaliana. Plant Physiology 170, 2478-2493

Liang G, Zhang H, Li X, *et al*. 2017. bHLH transcription factor bHLH115 regulates iron homeostasis in Arabidopsis thaliana. Journal of experimental botany 68, 1743-1755

Lichtenthaler HK. 1987. Chlorophylls and carotenoids: pigments of photosynthetic biomembranes. Methods in enzymology 148, 350-382

Long TA, Tsukagoshi H, Busch W, *et al*. 2010. The bHLH Transcription Factor POPEYE Regulates Response to Iron Deficiency in Arabidopsis Roots. Plant Cell 22, 2219-2236

Marschner H, Römheld V, Kissel M. 1986. Different strategies in higher plants in mobilization and uptake of iron. Journal of plant nutrition 9, 695-713

Mendoza-Cózatl DG, Xie Q, Akmakjian GZ, *et al*. 2014. OPT3 is a component of the iron-signaling network between leaves and roots and misregulation of OPT3 leads to an

over-accumulation of cadmium in seeds. Molecular plant 7, 1455-1469

Nakagawa T, Kurose T, Hino T, *et al.* 2007. Development of series of gateway binary vectors, pGWBs, for realizing efficient construction of fusion genes for plant transformation. Journal of bioscience and bioengineering 104, 34-41

Norkunas K, Harding R, Dale J, *et al.* 2018. Improving agroinfiltration-based transient gene expression in Nicotiana benthamiana. Plant methods 14, 71

Robe K, Conejero G, Gao F, *et al.* 2021a. Coumarin accumulation and trafficking in Arabidopsis thaliana: a complex and dynamic process. New Phytologist 229, 2062-2079

Robe K, Izquierdo E, Vignols F, *et al.* 2021b. The Coumarins: Secondary Metabolites Playing a Primary Role in Plant Nutrition and Health. Trends in Plant Science 26, 248-259

Robinson NJ, Procter CM, Connolly EL, *et al.* 1999. A ferric-chelate reductase for iron uptake from soils. Nature 397, 694-697

Santi S, Schmidt W. 2009. Dissecting iron deficiency‐induced proton extrusion in Arabidopsis roots. New Phytologist 183, 1072-1084

Stacey MG, Patel A, McClain WE, *et al.* 2008. The Arabidopsis AtOPT3 protein functions in metal homeostasis and movement of iron to developing seeds. Plant physiology 146, 589-601

Tanabe N, Noshi M, Mori D, *et al.* 2019. The basic helix-loop-helix transcription factor, bHLH11 functions in the iron-uptake system in Arabidopsis thaliana. Journal of plant research 132, 93-105

Terry N. 1980. Limiting factors in photosynthesis: I. Use of iron stress to control photochemical capacity in vivo. Plant Physiology 65, 114-120

Tissot N, Robe K, Gao F, *et al.* 2019. Transcriptional integration of the responses to iron availability in Arabidopsis by the bHLH factor ILR3. New Phytologist 223, 1433-1446

Vert G, Grotz N, Dédaldéchamp F, *et al.* 2002. IRT1, an Arabidopsis transporter essential for iron uptake from the soil and for plant growth. The Plant Cell 14, 1223-1233

Wang H-Y, Klatte M, Jakoby M, *et al.* 2007. Iron deficiency-mediated stress regulation of four subgroup Ib BHLH genes in Arabidopsis thaliana. Planta 226, 897-908

Wang N, Cui Y, Liu Y, *et al.* 2013. Requirement and functional redundancy of Ib subgroup bHLH proteins for iron deficiency responses and uptake in Arabidopsis thaliana.

Molecular plant 6, 503-513

Waters BM, Chu H-H, DiDonato RJ, *et al*. 2006. Mutations in Arabidopsis yellow stripe-like1 and yellow stripe-like3 reveal their roles in metal ion homeostasis and loading of metal ions in seeds. Plant Physiology 141, 1446-1458

Yi Y, Guerinot ML. 1996. Genetic evidence that induction of root Fe (III) chelate reductase activity is necessary for iron uptake under iron deficiency. The Plant Journal 10, 835-844

Yuan Y, Wu H, Wang N, *et al*. 2008. FIT interacts with AtbHLH38 and AtbHLH39 in regulating iron uptake gene expression for iron homeostasis in Arabidopsis. Cell research 18, 385-397

Yuan YX, Zhang J, Wang DW, *et al*. 2005. AtbHLH29 of Arabidopsis thaliana is a functional ortholog of tomato FER involved in controlling iron acquisition in strategy I plants. Cell research 15, 613-621

Zhai Z, Gayomba SR, Jung H-i, *et al*. 2014. OPT3 is a phloem-specific iron transporter that is essential for systemic iron signaling and redistribution of iron and cadmium in Arabidopsis. The Plant Cell 26, 2249-2264

Zhang J, Liu B, Li M, *et al*. 2015. The bHLH transcription factor bHLH104 interacts with IAA-LEUCINE RESISTANT3 and modulates iron homeostasis in Arabidopsis. The Plant Cell 27, 787-805

Figure legends

Fig. 1. *Arabidopsis thaliana* **bhlh121 and clade IVc bHLH double mutants display enhanced growth defects compare to** *bhlh121* **single mutants.** (**A**) Phenotype of wild type (WT), *bhlh121*, *bhlh34*, *bhlh104*, *bhlh105* and *bhlh115* loss-of-function mutants and *bhlh121 bhlh34*, *bhlh121 bhlh104*, *bhlh121 bhlh105* and *bhlh121 bhlh115* double mutants grown in soil for 5 weeks and watered or not with Fe-EDDHA (a form of Fe easily assimilated by plants). (**B**) Chlorophyll content in leaves of plants described in (A). (**C**) Iron concentrations in leaves of plants described in (A) grown in the absence of Fe-EDDHA. (**B-C**) Means within each condition with the same letter are not significantly different according to one-way ANOVA followed by post hoc Tukey test ($p \leq 0.05$). Means pairwise comparison were achieved using Student's *t*-test (**: $p \leq 0.01$). n = 3 biological repeats from one representative experiment. Error bars show ±SD. A biological repeat comprised about 20 mg of fresh leaves (B) or 10 mg of dried leaves (C) from one individual plant.

Fig. 2. Iron concentrations in the leaves and wild type (WT), *bhlh121*, *bhlh34*, *bhlh115*, *bhlh121 bhlh34* **and** *bhlh121 bhlh115* **plants.** The different *Arabidopsis thaliana* genotypes were grown in hydroponic culture in the presence of 50 µM Fe (control condition) for 5 weeks and then subjected to iron deficiency (0 µM Fe) or control (50 µM Fe) conditions for one week. Means within each condition with the same letter are not significantly different according to one-way ANOVA followed by post hoc Tukey test ($p \leq 0.05$). Means pairwise comparison were achieved using Student's *t*-test (**: $p \leq 0.01$). n = 3 biological repeats from one representative experiment. Error bars show ±SD. A biological repeat comprised about 10 mg of dried leaves from one individual plant.

Fig. 3. Expression of Fe-deficiency-responsive genes in wild type and bhlh121 and clade IVc single and double loss-of-function mutants grown under iron deficiency condition. Relative expression was determined by RT-qPCR in 7-day-old *Arabidopsis thaliana* seedlings grown under Fe-deficient (MS/2 medium). Means within each condition with the same letter are not significantly different according to one-way ANOVA followed by post hoc Tukey test ($p \leq 0.05$). Means pairwise comparison were achieved using Student's *t*-test (**: $p \leq 0.01$). n = 3 technical repeats from one representative experiment. Error bars show ±SD. Each experiment (biological repeat) comprised pooled RNA extracted from about 30 seedlings and was independently repeated three times.

Fig. 4. Overexpression of *bHLH34* and *bHLH105* partly rescue the growth defect of *bhlh121* mutant. (**A**) Phenotype of *Arabidopsis thaliana* wild type (WT), *bhlh121* and *bhlh121* mutant overexpressing clade IVc bHLH TFs. Plants were grown in soil for 4 weeks. (**B**). Chlorophyll content of plants described in (A). Means within each condition with the same letter are not significantly different according to one-way ANOVA followed by post hoc Tukey test ($p \leq 0.05$). n = 3 biological repeats from one representative experiment. Error bars show ±SD. A biological repeat comprised about 20 mg of fresh leaves from one individual plant.

Fig. 5. Overexpression of *bHLH34* and *bHLH105* in *bhlh121* increases the concentration of iron. (**A**) Iron concentrations in the leaves and roots of *Arabidopsis thaliana* plants grown under control hydroponic conditions (50 μM Fe) for 5 weeks and then subjected to either iron deficiency (0 μM Fe) or iron sufficiency (50 μM Fe) for one week. (**B**) Ferric-chelate reductase activity corresponding to the plants described in A that were submitted to iron deficiency. (**A-B**) Means within each condition with the same letter are not significantly different according to one-way ANOVA followed by post hoc Tukey test ($p \leq 0.05$). Means pairwise comparison were achieved using Student's *t*-test (**: $p \leq 0.01$). n = 3 biological repeats from one representative experiment. Error bars show ±SD. A biological repeat comprised about 10 mg of dried leaves (A) or 10 mg of fresh root tissues (B) from one individual plant.

Fig. 6. Expression of Fe-deficiency-responsive genes in wild type (WT), *bhlh12*1 and *bhlh12*1 mutant lines overexpressing clade IVc bHLH transcription factors grown under iron deficiency conditions. Relative expression was determined by RT-qPCR on 6-day-old *Arabidopsis thaliana* seedlings grown on Fe-deficient (0 μM Fe) MS/2 medium. Means within each condition with the same letter are not significantly different according to one-way ANOVA followed by post hoc Tukey test ($p \leq 0.05$). Means pairwise comparison were achieved using Student's *t*-test (**: $p \leq 0.01$). n = 3 technical repeats from one representative experiment. Error bars show ±SD. Each experiment (biological repeat) comprised pooled RNA extracted from about 30 seedlings and was independently repeated three times.

Fig. 7. GUS staining of *ProbHLH121:gbHLH121-GUS, ProbHLH34:gbHLH34-GUS, ProbHLH104:gbHLH104-GUS, ProbHLH105:gbHLH105-GUS* and *ProbHLH115:gbHLH115-GUS* transgenic plants. *Arabidopsis thaliana* seedlings were

grown on Fe sufficient MS/2 medium (50 μM Fe) and then were transferred to iron deficiency condition (0 μM Fe) for one week. Panels displaying whole seedlings are composite images combining 3 pictures. Zone I: root area below the hypocotyl; Zone II: root area with fully developed lateral roots; Zone III: root maturation zone; Zone IV: root tips and elongation zone.

Fig. 8. Clade IVc bHLH TFs act redundantly to target bHLH121 into the nucleus. (A) Co-transfection experiments between bHLH121-GFP and bHLH105-RFP or bHLH115-RFP in tobacco epidermal cell. n: nucleus, c: cytoplasm. Bars = 20 μ m. (**B**) bHLH121-GFP localization in the *Arabidopsis thaliana bhlh105* and *bhlh115* single loss-of-function mutants. Green: GFP, purple: cell walls labeled with propidium iodide. Bars = 20 μm. (**C**) Co-localization study of bHLH121-RFP and bHLH105-GFP or bHLH115-GFP in *Arabidopsis thaliana* roots. Bars = 20 μm.

Fig. 9. Regulation of *FIT* and clade Ib bHLH TFs expression by bHLH121 and clade IVc bHLH TFs to modulate Fe uptake. The expression of Fe uptake genes such as *IRT1* is directly controlled by the activity of FIT-dependent complexes involving clade Ib bHLH TFs such as bHLH39. bHLH121 acts upstream from the Fe homeostasis regulatory network by forming heterodimers with clade IVc bHLH TFs (green lines) to activate the expression of genes encoding several regulatory proteins, including *FIT* (indirect) and clade Ib bHLH TFs (direct). In the present study, we found that clade IVc bHLH TFs can activate the expression of clade Ib bHLH TFs independently of bHLH121 (orange lines); however, bHLH121 is indispensable for the activation of *FIT* expression by bHLH104 and bHLH115. The data also support the dual function of clade IVc bHLH TFs: (i) the regulation of the expression of *FIT* (indirect) and clade Ib bHLH TFs and (ii) the translocation of bHLH121 into the nucleus.
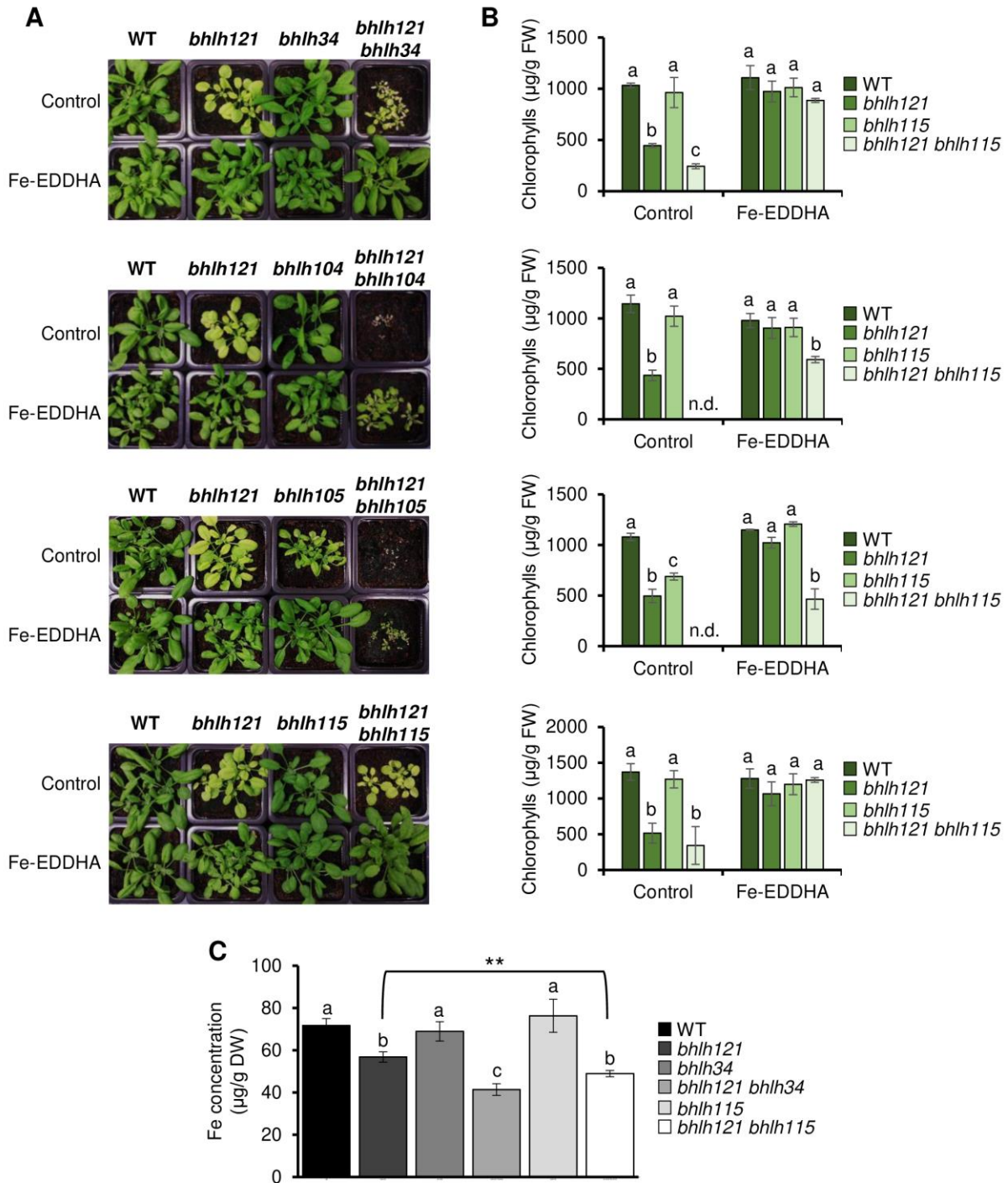
Figure 1. *Arabidopsis thaliana bhlh121* **and clade IVc bHLH double mutants display enhanced growth defects compare to** *bhlh121* **single mutants.** (**A**) Phenotype of wild type (WT), *bhlh121*, *bhlh34*, *bhlh104*, *bhlh105* and *bhlh115* loss-of-function mutants and *bhlh121 bhlh34*, *bhlh121 bhlh104*, *bhlh121 bhlh105* and *bhlh121 bhlh115* double mutants grown in soil for 5 weeks and watered or not with Fe-EDDHA (a form of Fe easily assimilated by plants). (**B**) Chlorophyll content in leaves of plants described in (A). (**C**) Iron concentrations in leaves of plants described in (A) grown in the absence of Fe-EDDHA. (**B-C**) Means within each condition with the same letter are not significantly different according to one-way ANOVA followed by post hoc Tukey test ($p \leq 0.05$). Means pairwise comparison were achieved using Student's *t*-test (**: $p \leq 0.01$). n = 3 biological repeats from one representative experiment. Error bars show $\pm$SD. A biological repeat comprised about 20 mg of fresh leaves (B) or 10 mg of dried leaves (C) from one individual plant.
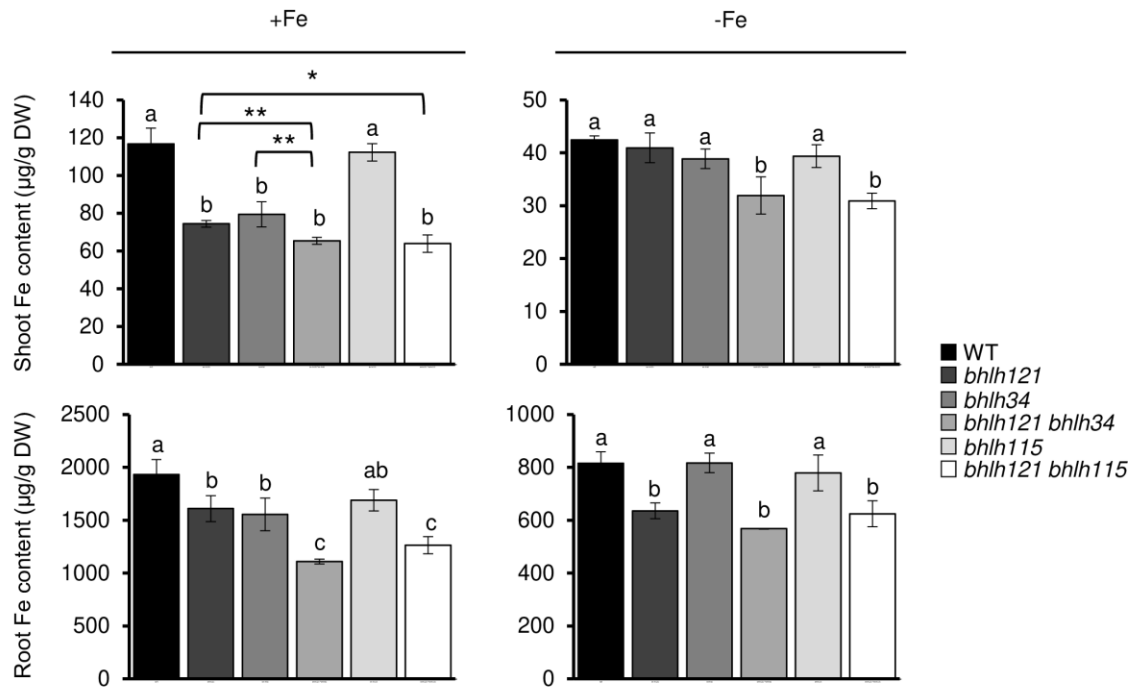
Figure 2. Iron concentrations in the leaves and wild type (WT), *bhlh121*, *bhlh34*, *bhlh115*, *bhlh121 bhlh34* and *bhlh121 bhlh115* plants. The different *Arabidopsis thaliana* genotypes were grown in hydroponic culture in the presence of 50 µM Fe (control condition) for 5 weeks and then subjected to iron deficiency (0 µM Fe) or control (50 µM Fe) conditions for one week. Means within each condition with the same letter are not significantly different according to one-way ANOVA followed by post hoc Tukey test ($p \leq 0.05$). Means pairwise comparison were achieved using Student's *t*-test (**: $p \leq 0.01$). n = 3 biological repeats from one representative experiment. Error bars show ±SD. A biological repeat comprised about 10 mg of dried leaves from one individual plant.

Figure 3. Expression of Fe-deficiency-responsive genes in wild type and bhlh121 and clade IVc single and double loss-of-function mutants grown under iron deficiency condition. Relative expression was determined by RT-qPCR in 7-day-old *Arabidopsis thaliana* seedlings grown under Fe-deficient (MS/2 medium). Means within each condition with the same letter are not significantly different according to one-way ANOVA followed by post hoc Tukey test ($p \leq 0.05$). Means pairwise comparison were achieved using Student's *t*-test (**: $p \leq 0.01$). n = 3 technical repeats from one representative experiment. Error bars show $\pm$SD. Each experiment (biological repeat) comprised pooled RNA extracted from about 30 seedlings and was independently repeated three times.

Figure 4. Overexpression of *bHLH34* and *bHLH105* partly rescue the growth defect of *bhlh121* mutant. (**A**) Phenotype of *Arabidopsis thaliana* wild type (WT), *bhlh121* and *bhlh121* mutant overexpressing clade IVc bHLH TFs. Plants were grown in soil for 4 weeks. (**B**). Chlorophyll content of plants described in (A). Means within each condition with the same letter are not significantly different according to one-way ANOVA followed by post hoc Tukey test ($p \leq$ 0.05). n = 3 biological repeats from one representative experiment. Error bars show $\pm$SD. A biological repeat comprised about 20 mg of fresh leaves from one individual plant.
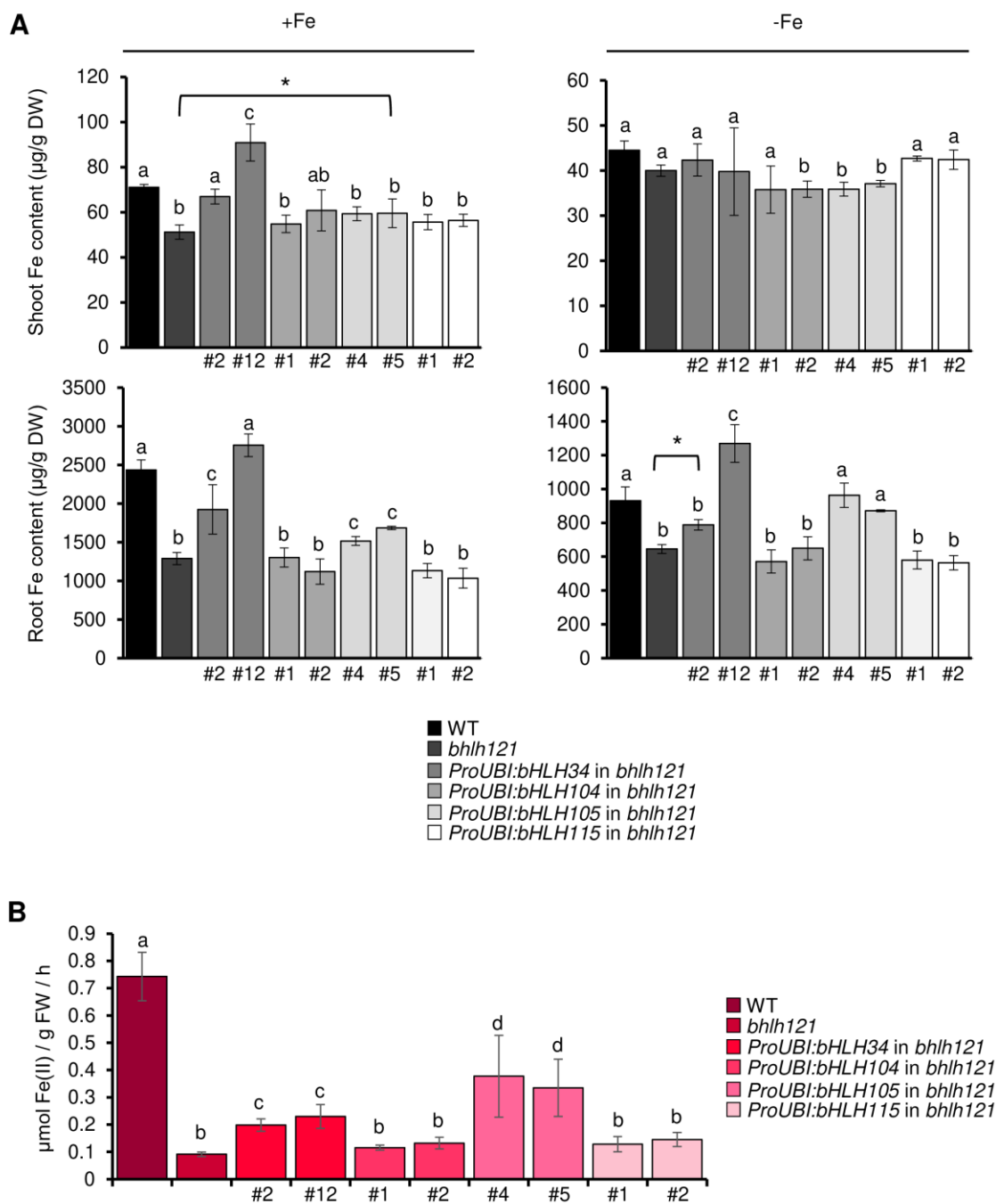
Figure 5. Overexpression of *bHLH34* and *bHLH105* in *bhlh121* increases the concentration of iron. (**A**) Iron concentrations in the leaves and roots of *Arabidopsis thaliana* plants grown under control hydroponic conditions (50 μM Fe) for 5 weeks and then subjected to either iron deficiency (0 μM Fe) or iron sufficiency (50 μM Fe) for one week. (**B**) Ferric-chelate reductase activity corresponding to the plants described in A that were submitted to iron deficiency. (**A-B**) Means within each condition with the same letter are not significantly different according to one-way ANOVA followed by post hoc Tukey test ($p \leq 0.05$). Means pairwise comparison were achieved using Student's *t*-test (**: $p \leq 0.01$). n = 3 biological repeats from one representative experiment. Error bars show ±SD. A biological repeat comprised about 10 mg of dried leaves (A) or 10 mg of fresh root tissues (B) from one individual plant.
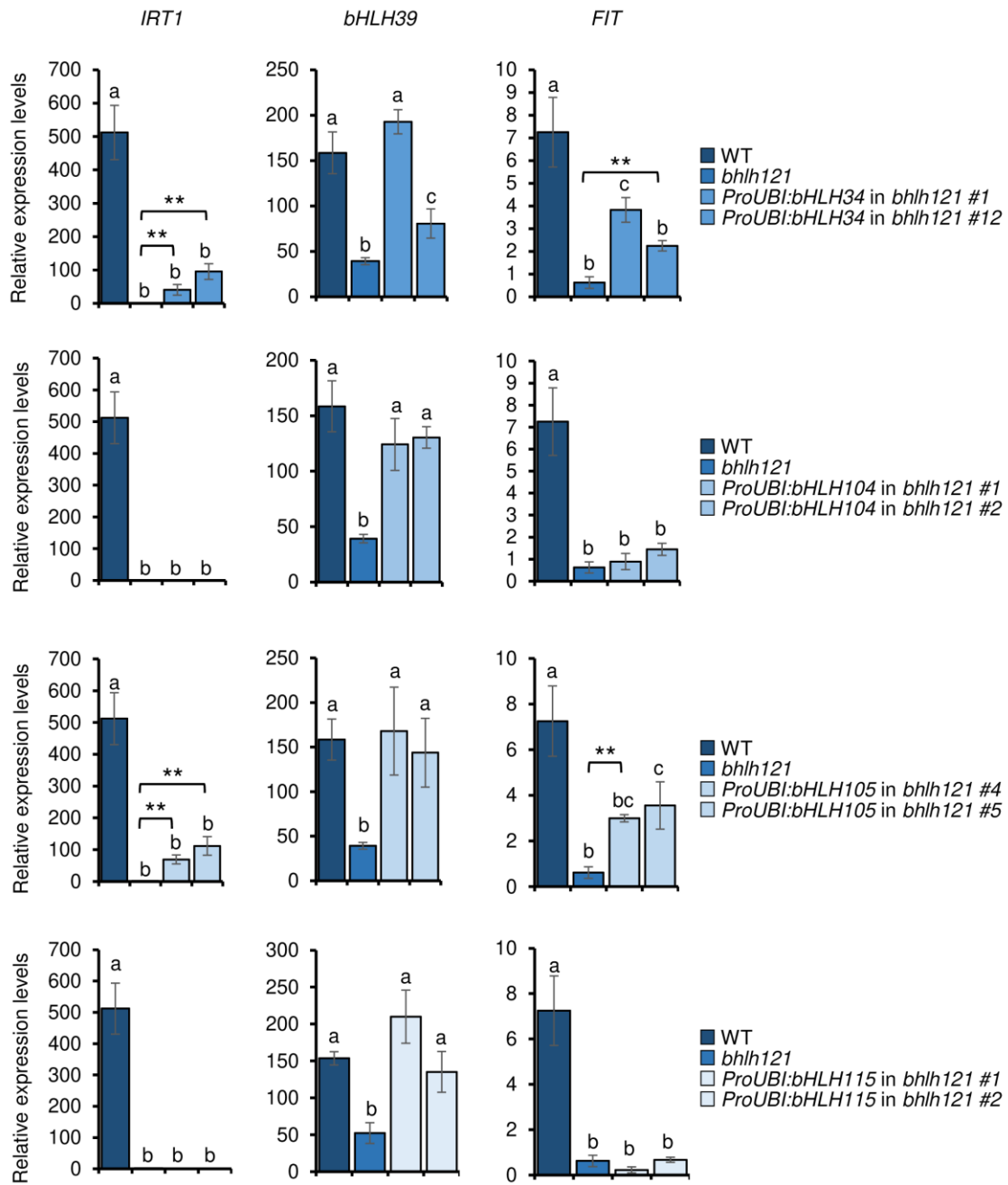
Figure 6. Expression of Fe-deficiency-responsive genes in wild type (WT), *bhlh121* and *bhlh121* mutant lines overexpressing clade IVc bHLH transcription factors grown under iron deficiency conditions. Relative expression was determined by RT-qPCR on 6-day-old *Arabidopsis thaliana* seedlings grown on Fe-deficient (0 µM Fe) MS/2 medium. Means within each condition with the same letter are not significantly different according to one-way ANOVA followed by post hoc Tukey test ($p \leq 0.05$). Means pairwise comparison were achieved using Student's *t*-test (**: $p \leq 0.01$). n = 3 technical repeats from one representative experiment. Error bars show ±SD. Each experiment (biological repeat) comprised pooled RNA extracted from about 30 seedlings and was independently repeated three times.
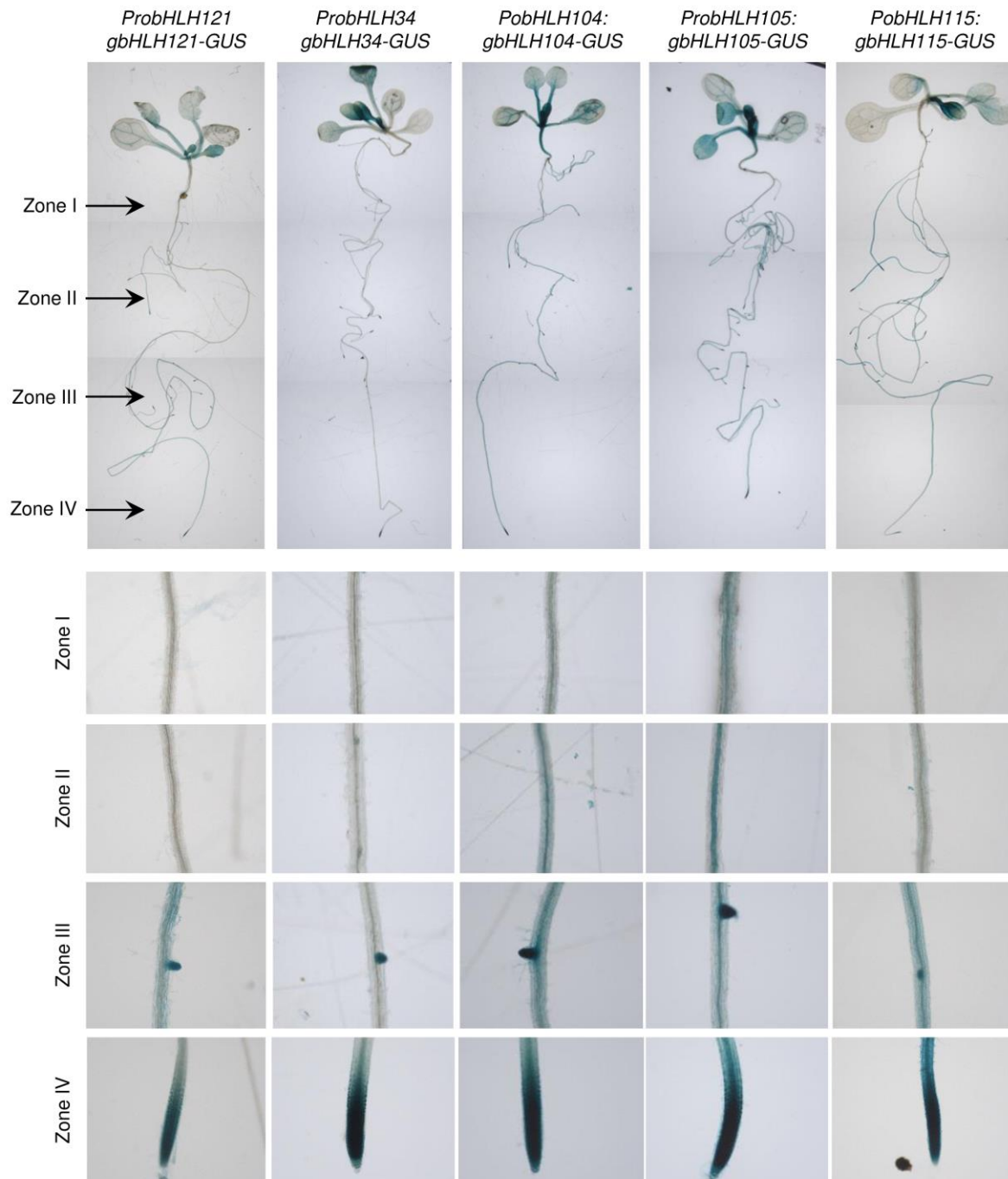
Figure 7. GUS staining of *ProbHLH121:gbHLH121-GUS, ProbHLH34:gbHLH34-GUS, ProbHLH104:gbHLH104-GUS, ProbHLH105:gbHLH105-GUS* and *ProbHLH115:gbHLH115-GUS* transgenic plants. *Arabidopsis thaliana* seedlings were grown on Fe sufficient MS/2 medium (50 µM Fe) and then were transferred to iron deficiency condition (0 µM Fe) for one week. Panels displaying whole seedlings are composite images combining 3 pictures. Zone I: root area below the hypocotyl; Zone II: root area with fully developed lateral roots; Zone III: root maturation zone; Zone IV: root tips and elongation zone.
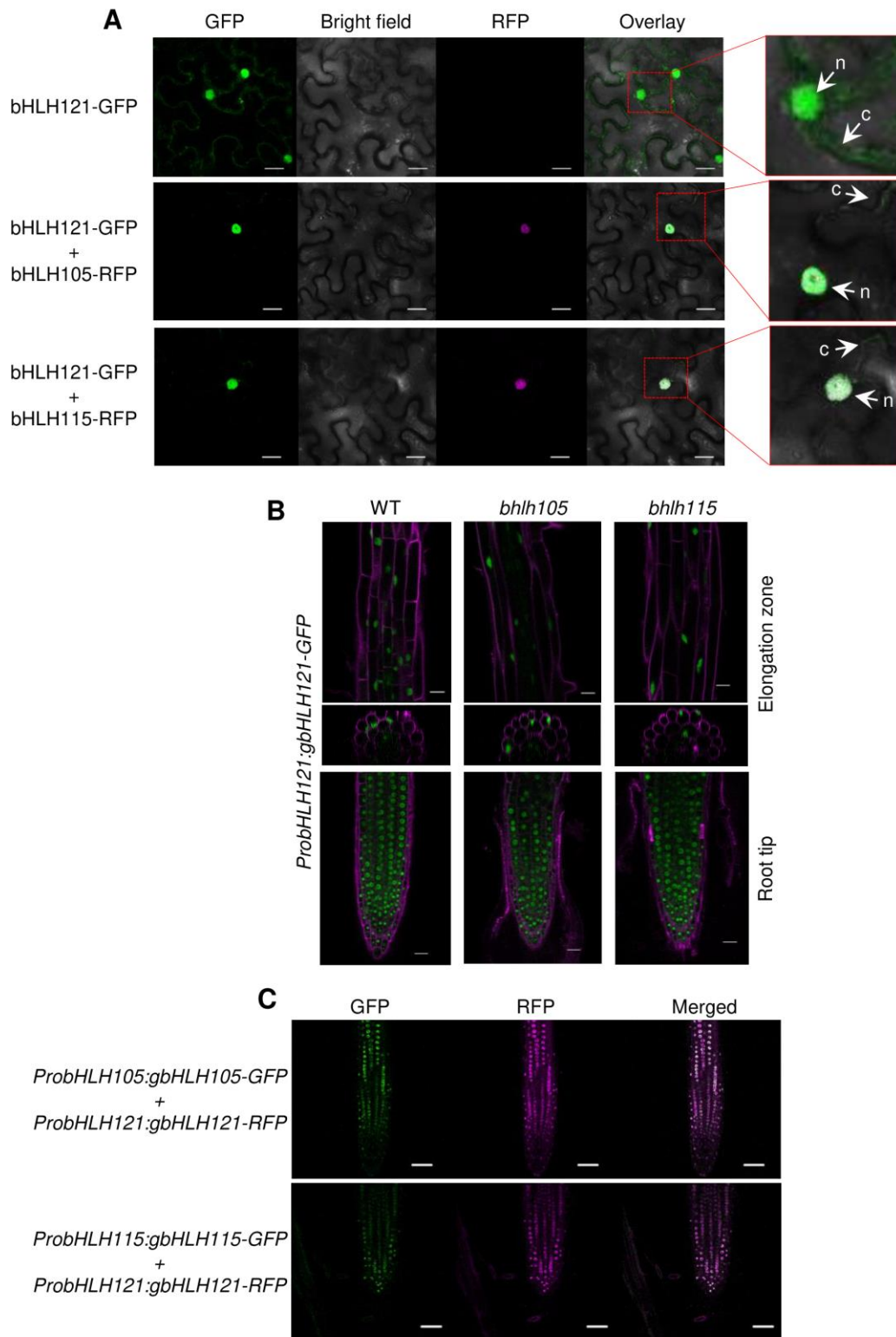
Figure 8. Clade IVc bHLH TFs act redundantly to target bHLH121 into the nucleus. (**A**) Co-transfection experiments between bHLH121-GFP and bHLH105-RFP or bHLH115-RFP in tobacco epidermal cell. n: nucleus, c: cytoplasm. Bars = xxx. (**B**) bHLH121-GFP localization in the *Arabidopsis thaliana bhlh105* and *bhlh115* single loss-of-function mutants. Green: GFP, purple: cell walls labeled with propidium iodide. Bars = 20 μm. (**C**) Co-localization study of bHLH121-RFP and bHLH105-GFP or bHLH115-GFP in *Arabidopsis thaliana* roots. Bars = 20 μm.
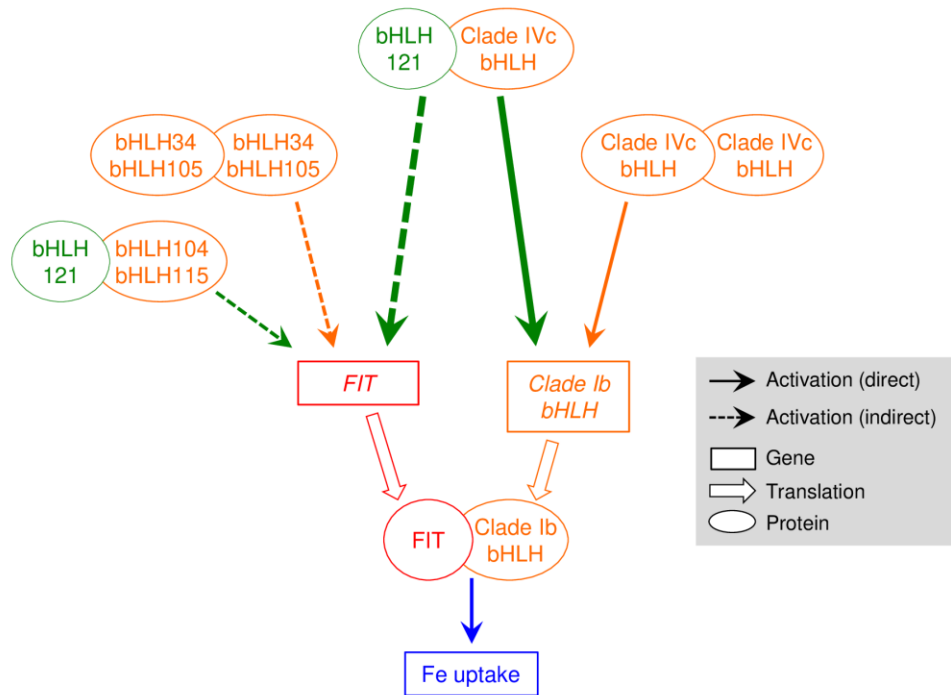
Figure 9. Regulation of *FIT* and clade Ib bHLH TFs expression by bHLH121 and clade IVc bHLH TFs to modulate Fe uptake. The expression of Fe uptake genes such as *IRT1* is directly controlled by the activity of FIT-dependent complexes involving clade Ib bHLH TFs such as bHLH39. bHLH121 acts upstream from the Fe homeostasis regulatory network by forming heterodimers with clade IVc bHLH TFs (green lines) to activate the expression of genes encoding several regulatory proteins, including *FIT* (indirect) and clade Ib bHLH TFs (direct). In the present study, we found that clade IVc bHLH TFs can activate the expression of clade Ib bHLH TFs independently of bHLH121 (orange lines); however, bHLH121 is indispensable for the activation of *FIT* expression by bHLH104 and bHLH115. The data also support the dual function of clade IVc bHLH TFs: (i) the regulation of the expression of *FIT* (indirect) and clade Ib bHLH TFs and (ii) the translocation of bHLH121 into the nucleus.